

# KINETICS OF THE MAIN PHASE TRANSITION OF HYDRATED LECITHIN MONITORED BY REAL-TIME X-RAY DIFFRACTION

MARTIN CAFFREY

*Section of Biochemistry, Molecular and Cell Biology, Clark Hall and Cornell High Energy Synchrotron Source (CHESS), Cornell University, Ithaca, New York 14853*

DONALD H. BILDERBACK

*Cornell High Energy Synchrotron Source (CHESS) and School of Applied and Engineering Physics, Cornell University, Ithaca, New York 14853*

**ABSTRACT** A method is described for observing and recording in real-time x-ray diffraction from an unoriented hydrated membrane lipid, dipalmitoylphosphatidylcholine (DPPC), through its thermotropic gel/liquid crystal phase transition. Synchrotron radiation from the Cornell High Energy Synchrotron Source (Ithaca, New York) was used as an x-ray source of extremely high brilliance and the dynamic display of the diffraction image was effected using a three-stage image intensifier tube coupled to an external fluorescent screen. The image on the output phosphor was sufficiently intense to be recorded cinematographically and to be displayed on a television monitor using a vidicon camera at 30 frames  $\cdot$  s<sup>-1</sup>. These measurements set an upper limit of 2 s on the DPPC gel  $\rightarrow$  liquid crystal phase transition and indicate that the transition is a two-state process. The real-time method couples the power of x-ray diffraction as a structural probe with the ability to follow kinetics of structural changes. The method does not require an exogenous probe, is relatively nonperturbing, and can be used with membranes in a variety of physical states and with unstable samples. The method has the additional advantage over its static measurement counterpart in that it is more likely to detect transiently stable intermediates if present.

As an x-ray source synchrotron radiation (SR) (1–5), which comes about as a result of the motion of relativistic charged particles in a curved path in a magnetic field, has been lauded for its inherent time structure, continuous wavelength spread, and extreme brilliance. Cornell High Energy Synchrotron Source (CHESS) (6), the SR facility used in the present study, operates in a mode parasitic to the high energy physics experiments carried out on the Cornell Electron Storage Ring (CESR). The extreme brilliance of SR is a consequence of the relativistic speed of the electrons that at CESR results in an angular divergence of the beam in the vertical of some 20 s of arc (0.0056°). In addition to this natural vertical collimation, the beam is horizontally focused at CHESS using a cylindrically bent single crystal (Fig. 1) providing a monochromatic (8.3 keV, 1.50 Å) beam with a focal spot size of  $\sim$ 1.5 mm<sup>2</sup>. It is the extreme brightness of this collimated x-ray source when used in conjunction with a suitable detection system that has made possible these real-time studies.

DPPC, the lipid used in the present series of experiments, consists of two identical long saturated hydrocarbon

chains and a head group with a permanent dipole moment. In the hydrated state, DPPC packs into bilayers with the hydrophobic acyl chains to the inside and the head group in the aqueous phase. Each bilayer is separated from the next by a layer of water. In excess water multilamellar vesicles form consisting of concentric spherical bilayers interspersed with layers of water in an onion skinlike arrangement (7).

Hydrated DPPC was employed in the present study and the x-ray diffraction pattern from these membranes identifies long (lattice type and symmetry) and short (hydrocarbon chain packing) range order within these structures (8–14) (Fig. 2 *A*). Low-angle ( $2\theta \leq 5^\circ$ ) reflections index according to a lamellar lattice and the magnitude of the lattice periodicity, which is a composite of lipid bilayer and interlamellar water layer thickness, varies depending on phase type, temperature, and degree of hydration (13–17). These factors also affect the wide-angle reflections that can be either diffuse and centered at  $(4.6 \text{ \AA})^{-1}$  when the lipid is in the liquid crystal phase or sharp at  $(4.2 \text{ \AA})^{-1}$  characteristic of gel phase lipid.

This communication documents the feasibility of observ-

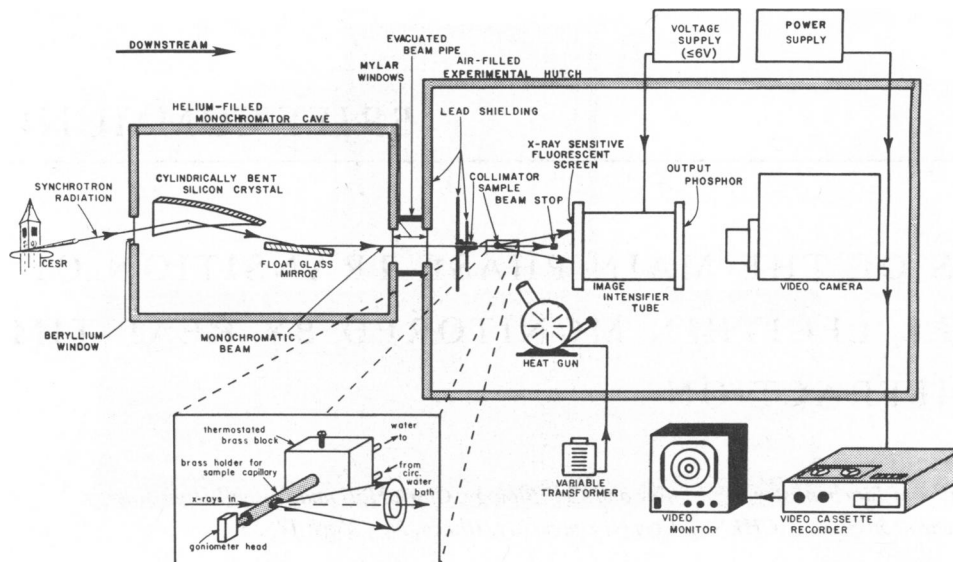


FIGURE 1 Schematic diagram of the experimental arrangement for monitoring x-ray diffraction from lipid samples in real time using synchrotron radiation (not drawn to scale). White light from CESR traverses an evacuated beam pipe (not shown) before entering the monochromator "cave," where it is simultaneously monochromatized and horizontally focused by a 10 cm long symmetric (111), triangular, cylindrically bent, single silicon crystal. Higher order harmonic contaminants from the focusing crystal are eliminated by total reflection of the fixed energy beam from a 30 cm long flat float glass mirror (27). In the experimental hutch the monochromatic beam was focused to a point  $\sim 1.5 \text{ mm}^2$ , 4.5 m from the silicon monochromator crystal and 7.4-cm downstream from the sample. X-rays diffracted from the sample were allowed to strike the zinc sulphide fluorescent screen on the frontplate of a three-stage intensifier tube (Varo image intensifier assembly, part No. 510-1267-403, operated at 6 V; Varo, Inc., Garland, TX) for image intensification (28). Dynamic display and recording of the image on the output phosphor of the intensifier tube was effected via a vidicon camera (Sony Corporation, Tokyo, Japan, AVC-1400), monitor (Hitachi-Denshi, Tokyo, Japan) and cassette recorder (Panasonic Omnivision II, VHS; Panasonic Co., Secaucus, NJ) assembly. DPPC samples in glass capillaries were placed in a tight-fitting brass holder and clamped in a brass block through which water from a thermostated water bath was circulated when required (see expanded view). This assembly was mounted on a goniometer head attached to a Buerger Precession Camera (Charles Supper, Co., Natick, MA; details not shown) that acted solely as an optical bench. For real time imaging a 1.3 mm (internal diameter) collimator (Charles Supper, Co.,) was used and the cassette carrier and drive mechanism was removed from the camera to allow positioning of the intensifier tube. Sample heating was effected by directing the sample hot air flow from a flameless heat gun, and a variable transformer was used to regulate air flow rate. For the duration of these experiments CESR was operated at an energy of 5.2 GeV in the single bunch mode with an electron beam current of 7–18 mA, a repetition rate of  $4 \times 10^5 \text{ Hz}$ , and a pulse size of  $\sim 130 \text{ ps}$ . Flux at the focal spot was  $3 \times 10^{10} \text{ photons/s}$  (5.2 GeV, 10 mA) measured with a 7.5 cm long  $\text{N}_2$ -filled ion chamber and a Keithley 427 amplifier (Keithley Instruments, Inc., Cleveland, OH) at a gain of  $10^7 \text{ V/A}$ . Flux was reduced  $\sim 35$ -fold by the 0.3 mm (internal diameter) collimator.

ing and recording in real-time changes in the x-ray diffraction of hydrated DPPC upon heating and cooling through the gel/liquid crystal phase transition temperature ( $T_i$ ). Heating was effected by directing hot air from a heat gun on the sample (Fig. 1) and cooling occurred in air when heating was terminated.

Changes in both low- and high-angle regions of the DPPC x-ray diffraction pattern were observed as they occurred in real time. This result is presented in Fig. 2. The diffraction pattern of one of the DPPC samples recorded on x-ray sensitive film following a 7-min exposure is included for comparative purposes (Fig. 2 A). The image intensifier used in these experiments accepts a cone of diffracted rays up to 40-mm diam. With the present experimental arrangement, therefore, it was not possible to simultaneously record with good resolution both low- and high-angle reflections. Accordingly, the two regimes were examined separately.

In Fig. 2 B the first order of the lamellar repeat from

DPPC multilayers at  $\sim 20\%$  (wt/wt) water is monitored through the  $T_i$ . As the sample is heated from room temperature ( $25^\circ\text{C}$ ) to above  $T_i$ , the sharp room temperature line at  $2\theta = 1.4^\circ$  ( $61 \text{ \AA}$ ) disappears and is concomitantly replaced by a distinctly resolved sharp reflection at  $2\theta = 1.6^\circ$  ( $54 \text{ \AA}$ ). For a limited time the two reflections coexist (Fig. 2 B, 2 and 3) but as sample temperature increases, the intensity of the  $1.6^\circ$  line grows at the expense of that at  $1.4^\circ$ . When the last trace of the  $1.4^\circ$  reflection has disappeared, the position of the high temperature line moves to higher angles in an apparently continuously manner and stabilized at  $2\theta = 1.82^\circ$  ( $47 \text{ \AA}$ ) as sample temperature increases and finally stabilizes. This sequence of events is reversed as the sample cools (Fig. 2 B, 5 and 6). Initially, there is a continuous decrease in the  $2\theta$  value of the high temperature line to  $1.6^\circ$  followed by a discontinuous jump in  $2\theta$  from  $1.6^\circ$  to  $1.4^\circ$  characteristic of the room temperature  $2\theta$  value. As with sample heating, coexistence of the  $1.4^\circ$  and  $1.6^\circ$  lines was observed for a finite time

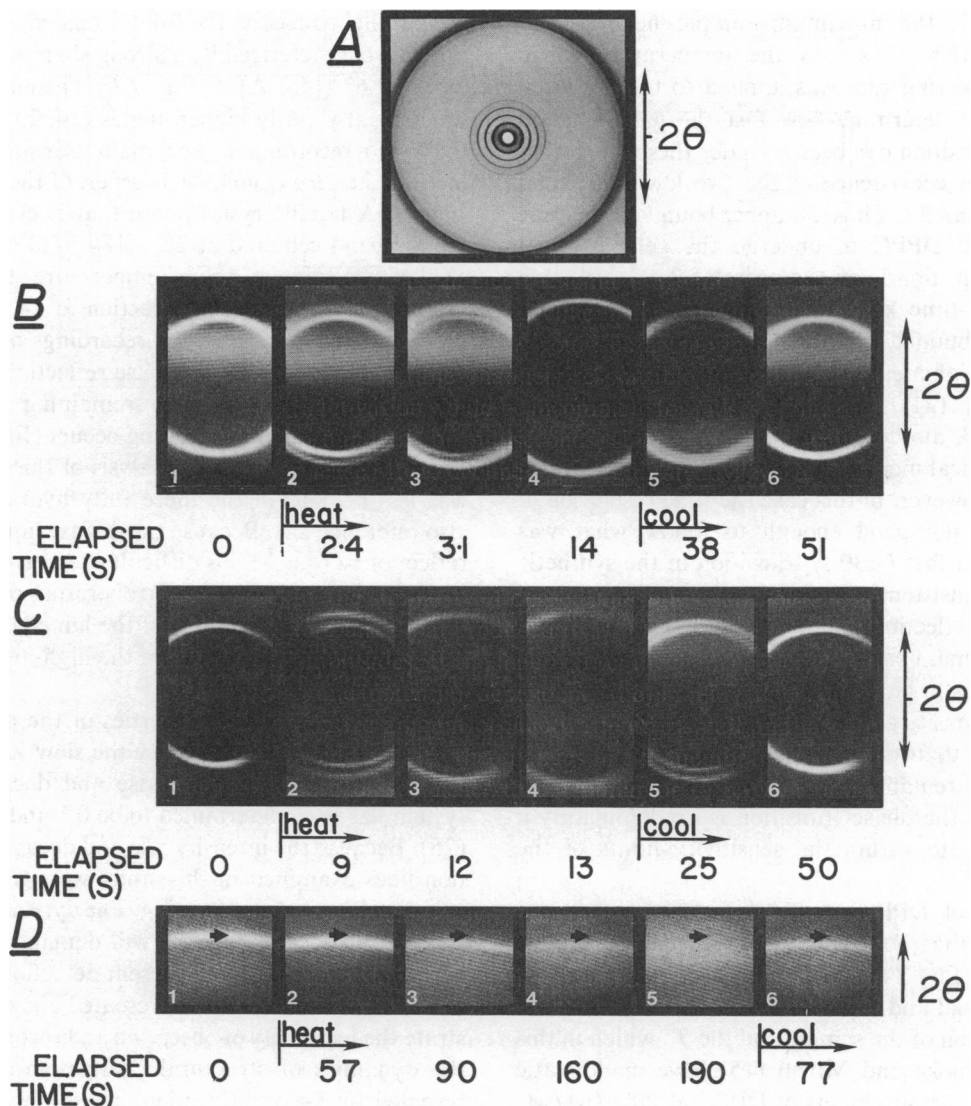


FIGURE 2 X-ray diffraction by hydrated DPPC recorded in real time and on x-ray sensitive film in static measurement. (A) Diffraction pattern of DPPC at ~25% (wt/wt) water recorded on CEA film (Reflex 25, CEA America Corp., Greenwich, CT) at 22°C following a 7-min exposure (5.2 GeV, 9 mA) with a 0.3 mm (internal diameter) collimator and sample-to-film distance of 75 mm. (B, C, D) Single frame photographs of real-time video recordings (30 frames/s) of x-ray diffraction by DPPC at ~20% (B) and ~10% (wt/wt) water (C, D) at low (B, C) and high-angle (D). The diffracted images were recorded in real time (see text and legend to Fig. 1 for details) through the  $T_i$  of the lipid using a 1.3-mm collimator. Elapsed time after the commencement of heating and cooling is indicated along with the direction of increasing diffraction angle, where according to Bragg:  $\sin \theta = n\lambda/2d$  (the integer,  $n$ , is the order of diffraction;  $\lambda$ , the x-ray wavelength (1.5 Å);  $d$ , the interplanar spacing; and  $\theta$ , the grazing angle of incidence). Detector-to-sample distance was ~40 cm (B, C) and 10 cm (D). Samples were prepared by incubating water and dried (from a chloroform solution) chromatographically pure DPPC (Avanti Polar Lipids, Inc., Birmingham, AL) in sealed ampoules above  $T_i$  and transferring the hydrated lipid to a glass capillary (Charles Supper, Co.) which was subsequently flame sealed (29). Different sample heating and cooling rates were used in B, C, and D. It was not intended, in this particular study, to examine or compare the temporality of changes in bilayer periodicity and chain packing. Sample decomposition was considered negligible since no difference was observed in the x-ray diffraction pattern recorded on x-ray sensitive film from a sample of DPPC with up to 1-h accumulated x-ray exposure (5.2 GeV, 7–18 mA).

during the cooling process. The coexistence of two low-angle reflections indicates phase coexistence assuming uniform sample heating. This phenomenon has been observed previously by x-ray diffraction in the static measurement mode for hydrated DPPC (18, 19). In a separate experiment the DPPC sample was incubated at a number of temperatures in the transition region. At each temperature the relative amounts of the two phases as

judged by real-time x-ray diffraction remained stable for up to 30 min. This result suggests that phase coexistence as observed in the temperature jump experiments did not arise from nonuniform sample heating nor from thermal gradients in the sample. In this regard note that the sample capillary is 1-mm diam and that similar results were obtained with a 0.3-mm diam collimator.

With the experimental arrangement as described in the

legend to Fig. 1, the maximum sample heating rate attainable was  $16^{\circ}\text{C} \cdot \text{s}^{-1}$  in the temperature range 30–70°C. This heating rate was applied to the hydrated DPPC sample to determine how fast the gel  $\rightarrow$  liquid crystal phase transition can occur. Under these conditions it was found that coexistence of the two low-angle lines lasted no more than 2 s. Thus, an upper bound on the time it takes hydrated DPPC to undergo the gel  $\rightarrow$  liquid crystal phase transition is on the order of 2 s. This value obtained by real-time x-ray diffraction is in agreement with the values obtained for hydrated dimyristoyl PC by a volume perturbation method (20) and for hydrated DPPC by pressure jump (21). X-ray diffraction has been used previously to look at the kinetics of phase transitions in model and biological membranes using a position-sensitive detector (22). However, in this case the time resolution of the system was not good enough to follow what was considered to be a fast ( $<30$  s) transition in the synthetic lipids, which is consistent with the present result.

The lamellar reflections from coexisting gel and liquid crystal phases remain sharp through the transition region with what appears to be a reciprocal relationship between the diffracted intensity of the two reflections. These observations indicate that the coherent domain size of the coexisting phases remains large throughout the transition and suggest that the phase transition is predominantly a two-state process to within the sensitivity limits of the real-time method.

The behavior of DPPC at  $\sim 10\%$  (wt/wt) water was quite similar to that of the more fully hydrated sample described above (Fig. 2 C). The only differences observed were in the original and final values of  $2\theta$  that reflect the degree of hydration of the sample and the  $T_i$ , which in this case is  $\sim 60^{\circ}\text{C}$ . Inoko and Mitsui (15) have made static x-ray diffraction measurements of DPPC at 20% (wt/wt) water at a number of temperatures above and below  $T_i$ . The behavior of this system was very similar to the results presented above in real-time in that a discontinuous jump of  $\sim 7$  Å in the lamellar d-spacing was observed at  $T_i$  followed by a continuous drop in d-spacing with increasing temperature above  $T_i$ .

Up to four orders of the primary low-angle reflection were observed in the original video display, and the temperature induced changes described above for the first-order reflection occurred simultaneously in each of the higher order lines. The heating and cooling cycle was repeated many times with what appeared to be identical behavior in the low-angle region in each cycle evidencing the thermodynamic reversibility of the transition at both levels of hydration. The existence of hysteresis loops was not investigated.

Changes in the high-angle diffraction lines of hydrated DPPC that reflect acyl chain packing and conformation were recorded in real time through  $T_i$  as depicted in Fig. 2 D. The low-temperature gel phase wherein the acyl chains

are parallel packed in the fully extended all-*trans* configuration is characterized by a strong sharp diffraction line at  $2\theta = 21.6^{\circ}$  ( $[4.2 \text{ \AA}]^{-1}$ ; Fig. 2 D, 1) and a weak diffuse shoulder at slightly higher angles (14, 23) (not obvious in the video recordings). The main transition represents a melting, i.e., *trans-gauche* disorder, of the acyl chains to a smectic A liquid crystal phase that is characterized by a diffuse band centered at  $2\theta = 18.8^{\circ}$  ( $[4.6 \text{ \AA}]^{-1}$ ; Fig. 2 D, 5). Upon cooling to room temperature, the diffuse band disappears as the sharp reflection at  $(4.2 \text{ \AA})^{-1}$  reforms. Note that in these real-time recordings of the 10% water sample the high-angle gel phase reflection moves to lower angles upon heating while remaining perfectly sharp before the actual chain melting occurs (Fig. 2 D, 1 and 4). Space does not permit an analysis of this behavior, which was less obvious in the more fully hydrated sample (see also reference 24). Because the diffuse liquid crystal phase reflection at  $(4.6 \text{ \AA})^{-1}$  is difficult to see using this real-time imaging system, evidence corroborating phase coexistence as observed in the behavior of the lamellar d-spacings was not immediately obvious from the high-angle region of the diffraction pattern.

The time resolution properties of the present real-time detection system is limited by the slow ZnS phosphors of the image intensifier. The rise and decay time for this system has been determined to be 0.1 and 1 s, respectively (25). Because the intensity rise and decay times of diffraction lines examined in this study were  $\geq 2$  s, instrument response time was not limiting. The dynamic display in real time of more rapid kinetics will demand improvement in the time resolution of the present detection system.

To conclude, the results presented above clearly demonstrate the feasibility of observing and recording in real time the dynamics of structural changes in lipid bilayers as revealed by x-ray diffraction. These measurements show that the characteristic time for the gel/liquid crystal phase transition of hydrated DPPC is  $\sim 2$  s and that the transition is predominantly a two-state process. The capability of making live-time measurements opens up numerous possibilities in the area of membrane biology. Imminently this potential will be further enhanced when CESR is operating with (a) multiple bunches of electrons, (b) a six-pole wiggler (26) situated immediately upstream from the focused x-ray beam, and (c) toroidal focusing optics. Taken together, a 500-fold increase in the diffracted x-ray intensity is anticipated as a result of these modifications. Such an improvement will allow for dynamic studies on dilute vesicle suspensions and possibly even isolated mono- and bimolecular lipid membranes where rapid mixing techniques can be used. In this way, the usefulness and versatility of SR as a probe of the structure and dynamics of model and biological membranes will be improved still further.

I thank G. W. Feigenson, G. P. Hess, Z. R. Korszun, and J. K. Moffat for their helpful criticism of this manuscript.

This study was supported in part by the National Institutes of Health, U. S. Public Health Service, under grant number HL-18255 to G. W. Feigenson.

Received for publication 20 September 1983.

## REFERENCES

1. Winick, H., and A. Bienenstock. 1978. Synchrotron radiation research. *Annu. Rev. Nucl. Part. Sci.* 28:33-113.
2. Barrington-Leigh, J., and G. Rosenbaum. 1976. Synchrotron x-ray sources: a new tool in biological structural and kinetic analysis. *Annu. Rev. Biophys. Bioeng.* 5:239-270.
3. Rowe, E. M., and J. H. Weaver. 1977. The uses of synchrotron radiation. *Sci. Am.* 236:32-41.
4. Rowe, E. M. 1981. Synchrotron radiation facilities in the United States. *Physics Today.* 34:38-37.
5. Winick, H., and S. Doniach. 1980. Synchrotron Radiation Research. Plenum Press, New York. 1-60.
6. Batterman, B., and N. W. Ashcroft. 1979. CHESS: The New Synchrotron Radiation Facility at Cornell. *Science (Wash. DC).* 206:157-161.
7. Bangham, A. D., M. W. Hill, and N. G. A. Miller. 1974. Preparation and use of liposomes as models of biological membranes. *Methods Membr. Biol.* 1:1-68.
8. Chapman, D., R. M. Williams, and B. D. Ladbrooke. 1967. Physical studies of phospholipids. VI. Thermotropic and lyotropic mesomorphism of some 1, 2-diacyl-phosphatidylcholines. *Chem. Phys. Lipids.* 1:445-475.
9. Tardieu, A., V. Luzzati, and R. C. Reman. 1973. Structure and polymorphism of the hydrocarbon chains of lipids: a study of lecithin-water phases. *J. Mol. Biol.* 75:711-733.
10. Ranck, J. L., L. Mateu, D. M. Sadler, A. Tardieu, T. Gulik-Krzywicki, V. Luzzati. 1974. Order-disorder conformational transitions of the hydrocarbon chains of lipids. *J. Mol. Biol.* 85:249-277.
11. Franks, N. P., and Y. K. Levine. 1981. Low-angle x-ray diffraction. *Mol. Biol. Biochem. Biophys.* 31:437-487.
12. Wilkins, M. H. F., A. E. Blaurock, D. M. Engelman. 1971. Bilayer structure in membranes. *Nature (Lond.).* 230:72-76
13. Luzzati, V. 1968. X-ray diffraction studies of lipid-water systems. In Biological Membranes, Physical Fact and Function. D. Chapman, editor. Academic Press, Inc., New York. 71-123.
14. Brady, G. W., and D. B. Fein. 1977. An analysis of the x-ray interchain peak profile in dipalmitoylglycerophosphocholine. *Biochim. Biophys. Acta.* 464:249-259.
15. Inoko, Y., and T. Mitsui. 1978. Structural parameters of dipalmitoyl phosphatidylcholine lamellar phases and bilayer phase transitions. *J. Physiol. Soc. Japan.* 44:1918-1924.
16. Small, D. M. 1967. Phase equilibria and structure of dry and hydrated egg lecithin. *J. Lipid Res.* 8:551-557.
17. Shipley, G. G. 1973. Recent x-ray diffraction studies of biological membranes and membrane components. In Biological Membranes. D. Chapman and D. F. H. Wallach, editors. Academic Press, Inc., New York. 1-89.
18. Gottlieb, M. H., and E. D. Eanes. 1974. Coexistence of rigid crystalline and liquid crystalline phases in lecithin-water mixtures. *Biophys. J.* 14:335-342.
19. Rand, R. P., D. Chapman, and K. Larsson. 1975. Tilted hydrocarbon chains of dipalmitoyl lecithin become perpendicular to the bilayer before melting. *Biophys. J.* 15:1117-1124.
20. Johnson, M., T. C. Winter, and R. L. Biltonen. 1983. The measurement of the kinetics of lipid phase transitions: a volume-perturbation kinetic calorimeter. *Anal. Biochem.* 128:1-6.
21. Yager, P., and W. L. Peticolas. 1982. The kinetics of the main phase transition of aqueous dispersions of phospholipids induced by pressure jump and monitored by Raman spectroscopy. *Biochim. Biophys. Acta.* 688:775-785.
22. Dupont, Y., A. Gabriel, M. Chabre, T. Gulik-Krzywicki, and E. Schechter. 1972. Use of a new detector for x-ray diffraction and kinetics of the ordering of the lipids in *E. coli* membranes and model systems. *Nature (Lond.).* 238:331-333.
23. Janiak, M. J., D. M. Small, and G. G. Shipley. 1976. Nature of the thermal pretransition of synthetic phospholipids: dimyristoyl- and dipalmitoyllecithin. *Biochemistry.* 21:4575-4580.
24. Furuya, K., and T. Mitsui. 1979. Phase transitions in bilayer membranes of dioleoyl-phosphatidylcholine/dipalmitoyl-phosphatidylcholine. *J. Physiol. Soc. Japan.* 46:611-616.
25. Caffrey, M., and D. H. Bilderback. 1983. Real-time x-ray diffraction using synchrotron radiation: system characterization and applications. *Nucl. Instrum. Meth.* 208:495-510.
26. Winick, H., G. Brown, K. Halbach, and J. Harris. 1981. Synchrotron radiation: wiggler and undulator magnets. *Physics Today.* 34:50-63.
27. Bilderback, D. H., and S. Hubbard. 1981. X-ray mirror reflectivities from 3.8 to 50 keV (3.3 to 0.25 Å). CHESS Technical Memorandum No. 12. Cornell University, Ithaca, New York. 1-23.
28. Green, R. E. 1971. Electro-optical systems for dynamic display of x-ray diffraction images. *Adv. X-Ray Anal.* 14:311-337.
29. Caffrey, M., and G. W. Feigenson. 1981. Fluorescence quenching in model membranes: relationship between calcium adenosinetriphosphatase enzyme activity and the affinity of the protein for phosphatidylcholines with different acyl chain characteristics. *Biochemistry.* 20:1949-1961.